Biochimica et Biophysica Acta, 895 (1987) 259–274
Elsevier

BBA 86153

Hypothesis

The molecular 'double-pivot' mechanism for water oxidation

George Christou and John B. Vincent

Department of Chemistry, Indiana University, Bloomington, IN (U.S.A.)

(Received 15 August 1988)

Contents

I. Introduction

The most important role yet recognized for manganese (Mn) in nature is its direct involvement in the photocatalytic, four-electron oxidation of water to O_2 within the photosynthetic apparatus of green plants and cyanobacteria. A total of four Mn atoms have been established as essential for O_2 evolution activity, and current evidence suggests that they are bound at or near the lumenal surface of the thylakoid membrane and near to the P-680 (PS II) reaction center [1–3]. It is currently believed that the Mn assembly is ligated to one or both of the membrane-bound polypeptides labeled D_1 and D_2 (which would correspond to the L and M polypeptides of the better-characterized bacterial reaction center of purple bacteria) and which probably bind the PS II chlorophyll groups and accessory components involved in the photochemistry and subsequent charge separation processes [4,5]. The Mn assem-

Abbreviations: py, pyridine; bipy, 2,2′-bipyridine; OAc, acetate anion; HIm, imidazole; EXAFS, extended X-ray absorption fine structure; μ_n-X, inorganic nomenclature indicating that ligand X is bridging n metal atoms (the subscript n may be omitted when $n = 2$); μ, magnetic moment, related to the square root of the magnetic susceptibility; PS II, Photosystem II.

Correspondence: G. Christou, Department of Chemistry, Indiana University, Bloomington, IN 47405, U.S.A.

bly functions as the electron donor to PS II via the intermediacy of Z, the EPR-detectable group which represents the direct-electron donor to P-680$^+$ (being converted to Z^+) and which is now believed to be the phenolic side-chain of Tyr-161 of polypeptide D_1 [6]. The function of the Mn assembly is, therefore, actually the re-reduction of Z^+ allowing further electron donation by the latter to the reaction center. The Mn assembly can provide a total of four electrons in four one-electron steps. When the fourth electron is donated, the Mn assembly is re-reduced to its lowest oxidation state by the four-electron oxidation of two water molecules (Eqn. 1), and is now

$$2H_2O \rightarrow O_2 + 4H^+ + 4e^- \quad (1)$$

ready for recycling. The Mn assembly can thus be considered as acting as a 'biological capacitor', capable of storing a total of four oxidizing equivalents before the 'capacitor' is discharged by oxidation of water. In this way, Nature has evolved a means of avoiding the generation of hydroxyl radicals. Since the PS II (P-680) photochemistry and subsequent charge separation involve a one-electron process, and the Z/Z^+ couple is also a one-electron process, direct use of water as the electron donor to Z would lead to generation of highly reactive hydroxyl radicals, a situation that a biological system would reasonably be expected to avoid (Eqn. 2). The intermediacy of the Mn

$$H_2O \rightarrow H^+ + HO^{\cdot} + e^- \quad (2)$$

thus allows storage of the oxidizing equivalents and subsequent oxidation of water by two two-electron or one four-electron steps, thus avoiding the generation of $HO^{\cdot}$. Also, of course, the metal site can function as the catalytic site, binding the substrate molecules and facilitating oxygen–oxygen bond formation.

The above general considerations define the overall function, but what is lacking at the present time is an understanding of the precise structure and mechanism of action of the Mn assembly at a molecular level, viz what is the precise structure of the Mn assembly and its ligands, and what is the precise mechanism by which it binds the substrate (H_2O) molecules and ultimately converts them to O_2? A number of such proposals have been published to date, but few of these have incorporated a three-dimensional structure for the Mn unit or been based on structural units known to exist in the inorganic chemistry of this metal [7,8].

As inorganic chemists, our contribution to this area has been the application of the inorganic model approach. This involves the synthesis and establishment of the exact structures and properties of Mn complexes capable of existence, and their use as a well-characterized and sound starting point to suggest by extrapolation what may be occurring within the biological system. An inherent belief in this approach is that the metal-containing unit in the biological system is capable of laboratory synthesis! Confidence that this is the case is provided by numerous studies with other metallobiomolecules which have shown that their metal units do not owe their absolute existence to the polypeptide environment in which they naturally reside, but instead represent thermodynamic minima of the constituent components. The argument on which our inorganic modeling approach is based is thus the logical inverse of this statement viz that the established thermodynamically stable synthetic complexes obtained in the laboratory from reaction mixtures containing the appropriate (biologically relevant) components may very well correspond to those in the native unit. The sequence of events in our modeling approach is thus the following: (i) establish and characterize the thermodynamically stable Mn complexes capable of existence; (ii) identify those that possess the appropriate properties (e.g., nuclearity, structural features, oxidation levels, etc.) to suggest that they may correspond to the biological unit; and (iii) employ them to propose the mechanism by which these complexes, when within the native system, could be carrying out the observed biological function, making sure that the proposal both makes 'inorganic' sense and is consistent with the various biochemical and biophysical data accumulated on the catalytic cycle.

Our inorganic modeling approach has recently provided a variety of synthetic materials which allow us to proceed to steps (ii) and (iii). In this respect, this paper represents a progress report of our approach and is by no means meant to be taken as the final story.

Our mechanistic hypothesis has already been briefly communicated [8]; we herein summarize our synthetic studies, and results therefrom, which led to the proposal being formulated, describe the latter in more detail, and discuss its potential relevance to the biological site by examining it in light of current data obtained from the variety of techniques employed in studying the native site. In addition, we shall suggest how the inorganic chemistry and the proposal itself can help explain or at least rationalize certain data on the native site which have proven difficult to interpret or, in some cases, interpret unambiguously.

II. Synthetic studies

Current evidence, much of which will be considered in subsequent sections, suggests the Mn assembly probably consists of a tetranuclear Mn_4 cluster bridged by an undetermined number of oxide (O^{2-}) groups and ligated predominantly by carboxylate side-chain functions of aspartate and glutamate, and possibly with imidazole and phenoxide ligation from histidine and tyrosine side-chains. The Mn cluster is capable of cycling through five oxidation levels labeled S_0–S_4, the last of which is unstable and spontaneously reverts to S_0 with evolution of O_2 [9].

$$S_0 \xrightarrow{-e^-} S_1 \xrightarrow{-e^-} S_2 \xrightarrow{-e^-} S_3 \xrightarrow{-e^-} S_4 \rightarrow S_0 + O_2$$

The Mn oxidation levels are believed to comprise combinations from the range II–IV. This suggested both the ligands and Mn oxidation levels to be employed in our inorganic modeling studies and, in particular, we have concentrated on employing simple organic carboxylic acids as 'substitutes' for aspartate and glutamate.

After preliminary experimentation, synthetic procedures have been developed leading to the desired complexes vis-à-vis nuclearity, oxide bridges and ligation type. Treatment of the trinuclear complexes $[Mn_3O(O_2CR)_6L_3]^{0,+}$ (R = various, L = py, H_2O) with three equivalents of the bidentate ligand bipyridine (bipy) leads to clean and high yield formation of the tetranuclear products $[Mn_4O_2(O_2CR)_6(bipy)_2]$ (1, R = Me) and $[Mn_4O_2(O_2CR)_7(bipy)_2]^{Z+}$ (2, Z = 0, R = Ph; 3, Z = 1, R = H, Me, Et, Ph) [10,11]. The structures of 1 and 3 (R = Me) have been determined by X-ray crystallography establishing the presence

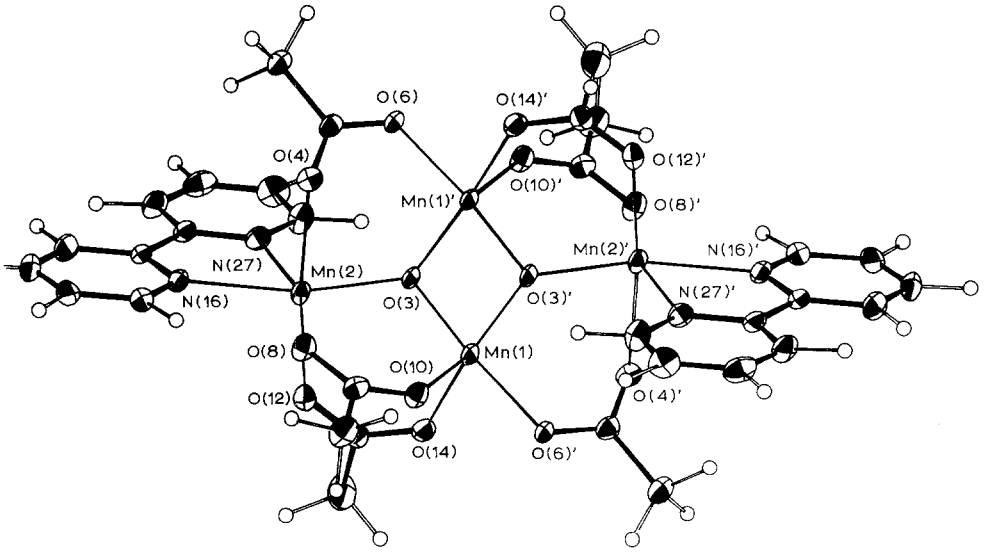

Fig. 1. The structure of $Mn_4O_2(O_2CMe)_6(bipy)_2$ (1). The primed and unprimed atoms are related by an imposed inversion center. Oxygen atoms O(3) and O(3)′ lie above and below the perfect Mn_4 plane. Mn(1) and Mn(1)′ are the Mn^{III} ions.

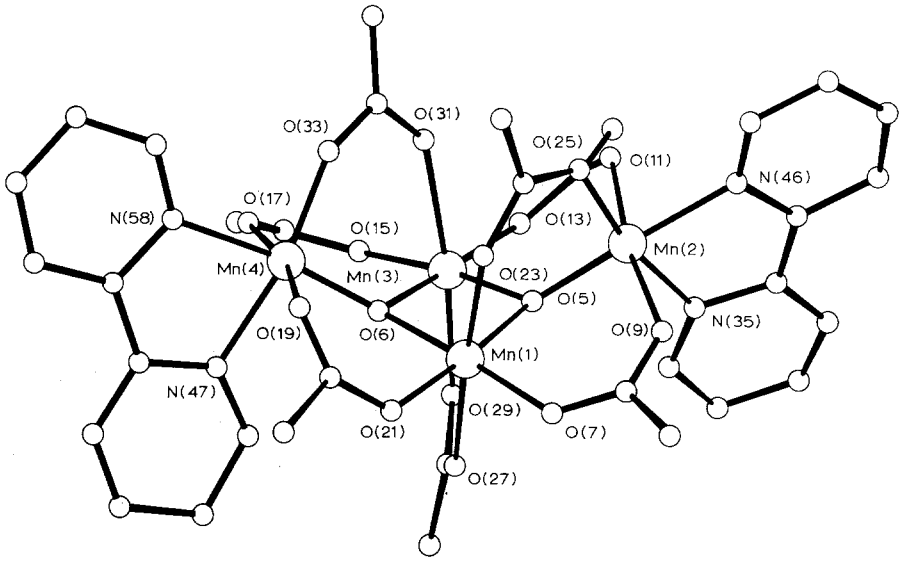

Fig. 2. The structure of $Mn_4O_2(O_2CMe)_7(bipy)_2^+$ (3), emphasizing the non-planar or 'butterfly' arrangement of the Mn_4 unit.

of the $Mn_4(\mu_3\text{-}O^{2-})_2$ central unit. The Mn_4 unit in 1 is planar (Fig. 1) whereas in 3 it adopts a 'butterfly' arrangement (Fig. 2) with Mn(1) and Mn(3) occupying the so-called 'hinge' or 'backbone' positions and Mn(2) and Mn(4) occupying 'wing-tip' positions. The complexes both possess two distinct Mn...Mn separations. In 3, the central Mn(1)...Mn(3) distance is 2.848 Å whereas the remaining Mn...Mn separations are in the range 3.299–3.385 Å. In 1, the two corresponding separations are 2.779 Å (Mn(1)...Mn(1)′) and 3.288–3.481 Å.

Complexes 1–3 contain average Mn oxidation levels of +2.5, +2.75 and +3.0, respectively; these of course arise from the individual oxidation state content of (2 Mn^{II}, 2 Mn^{III}), (Mn^{II}, 3 Mn^{III}) and (4 Mn^{III}). Based on S_1 containing all Mn^{III} centers, the oxidation state correspondence with the S_n states would be that depicted below:

$Mn_4O_2(O_2CR)_6(bipy)_2$ $\quad$ $Mn_4O_2(O_2CR)_7(bipy)_2$

$2Mn^{II}, 2Mn^{III}$ $\quad$ $Mn^{II}, 3Mn^{III}$

S_{-1} $\quad$ S_0

$Mn_4O_2(O_2CR)_7(bipy)_2^+$

$4Mn^{III}$

S_1

S_{-1} is the most reduced, stable state accessible, but it does not participate in the catalytic cycle (vide infra). It is our submission that the $[Mn_4O_2]$-containing products may represent models of the lower S_n states of the native site. If this is entertained, an important question to be addressed is whether the synthetic materials display the appropriate electrochemical interconversions required of these S_n states during turnover. An investigation by the cyclic voltammetric technique has indeed established the presence of reversible, one-electron couples, as summarized in the two electron-transfer equations below where equivalent oxidation levels are presented in the same column.

$$[]^- \quad \leftarrow [] \rightleftarrows [Mn_4O_2(O_2CR)_7(bipy)_2]^+ \rightleftarrows []^{2+}$$

$$\underline{2} \qquad\qquad \underline{3}$$

$$[Mn_4O_2(O_2CR)_6(bipy)_2] \rightleftarrows []^+$$

$$\underline{1}$$

$$S_{-1} \qquad S_0 \qquad S_1 \qquad S_2$$

Thus, the proposed S_1 model complex 3 displays an electrochemically quasi-reversible reduction to complex 2; inversely, complex 2 shows an identical process but in the opposite direction. Reduction of 2 to the S_{-1} oxidation level is both electrochemically irreversible and at a quite negative potential. It is perhaps not surprising, therefore, that the isolated S_{-1} model is of a different for-

mulation, viz with only six RCO_2^- ligands; this, in turn, can be electrochemically converted by a reversible one-electron process to $[Mn_4O_2(O_2CR)_6(bipy)_2]^+$, currently not obtained in an isolated form. Overall, then, the three isolated oxidation levels of the Mn_4O_2 complexes are electrochemically interconvertible, albeit with a slight adjustment of the ligand-to-metal ratio being required for a stable S_{-1} model complex.

The S_1 model complex 3 also displays a quasi-reversible, one-electron process yielding $[Mn_4O_2(O_2CR)_7(bipy)_2]^{2+}$. This would correspond to the S_2 state. Although this oxidation level of the synthetic species has yet to be isolated, its detection is important in considerations to be discussed below.

Continued synthetic investigation eventually led to tetranuclear complexes possessing the average Mn oxidation level (+3.25; $3Mn^{III}$, Mn^{IV}) believed to correspond to S_2; however, these products were of a structure different from putative $[Mn_4O_2(O_2CR)_7(bipy)_2]^{2+}$ detected electrochemically. The first such species was $[Mn_4O_3Cl_6(OAc)_3(HIm)]^{2-}$ (4, HIm = imidazole) depicted in Fig. 3 [12]. Other forms of this material have since been obtained viz $Mn_4O_3Cl_4(OAc)_3(py)_3$ (5) and $Mn_4O_3Cl_4(OAc)_3(HIm)_3$ (6) (Ref. 14; see also Li, Q., Boyd, P.W., Hendrickson, D.N., Vincent, J.B., Libby, E. and Christou, G., unpublished results). These all contain a Mn_4 tetrahedron with the Mn^{IV} in the apex. A Cl^- bridges the basal face whereas an O^{2-} bridges each of the three vertical faces. An acetate group bridges each Mn^{IV}–Mn^{III} edge, and ligation at the three Mn^{III} sites is completed by various combinations of terminal Cl^- and terminal HIm or py groups (leading to the three different complexes 4–6). As for the $[Mn_4O_2]$-containing species, Mn ... Mn separations fall into two distinct types. The Mn^{IV}... Mn^{III} separations are approx. 2.8 Å, whereas Mn^{III}... Mn^{III} separations are approx. 3.3 Å. Complexes 4–6 display no reversible processes when examined by the cyclic voltammetry technique.

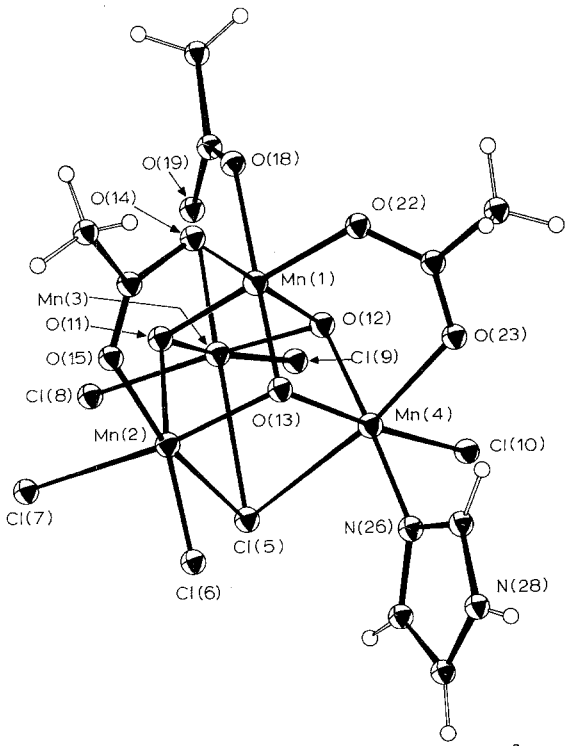

Fig. 3. The structure of $[Mn_4O_3Cl_6(O_2CMe)_3(HIm)]^{2-}$ (4). Mn(1) is the Mn^{IV} ion.

It is interesting to note that the $[Mn_4O_3]$ core of 4–6 is more structurally related to the Mn_4O_2 core than might at first glance seem apparent. The Mn_4O_3 core can be obtained from the Mn_4O_2 butterfly unit by merely placing a third μ_3-O^{2-} to bridge between the two 'wing-tip' and one of the 'hinge' Mn sites, as shown below:

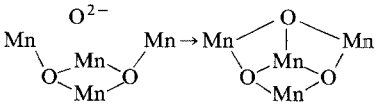

This again will be important to later discussion.

III. The 'double-pivot' mechanism

We will now describe how the results of the synthetic studies summarized above can be employed to formulate our mechanistic proposal for the water-oxidation cycle. The proposal is depicted in schematic form (Scheme I) in Fig. 4 [8]; for clarity, the peripheral ligation is not shown. At S_0, we place the Mn_4O_2 unit established in complex 2. A one-electron oxidation converts this to S_1, where we also depict a Mn_4O_2 unit as we found in complex 3; remember that electrochemical conversion of 2 to 3 was established, as described earlier. On oxidation of S_1 to S_2, the same Mn_4O_2 unit is retained, but now the two substrate

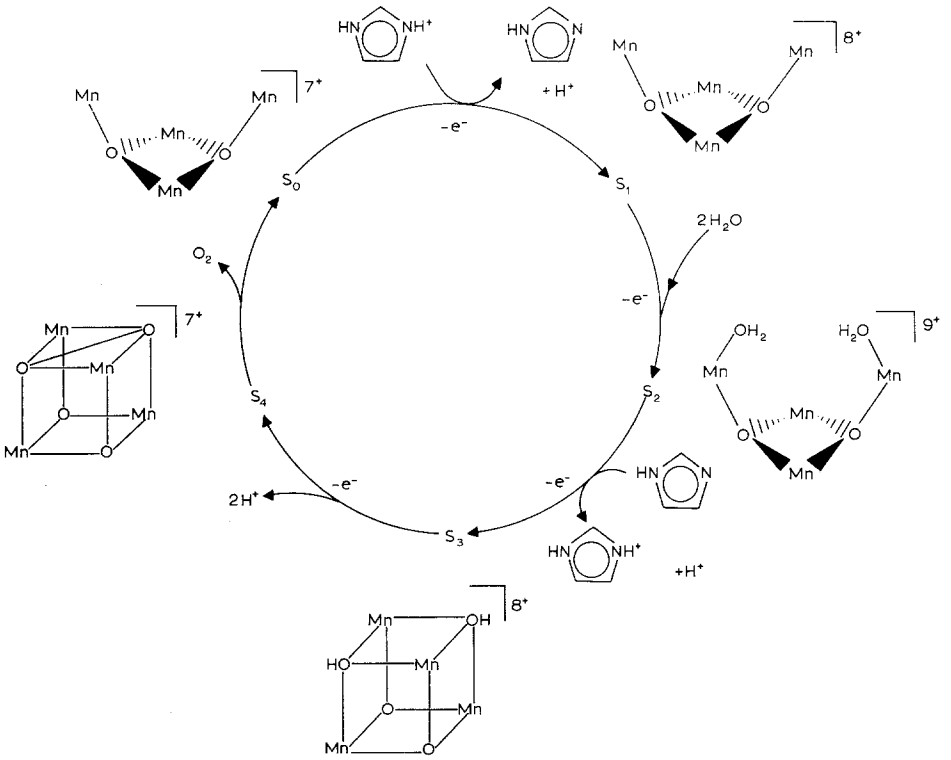

Fig. 4. Mechanistic proposal for the water oxidation cycle; referred to as Scheme I in the text.

water molecules are indicated as bound to the two 'wing-tip' Mn atoms (we do not imply that they are not bound at S_1, necessarily, only that they are bound by S_2). Note that electrochemical generation of the Mn_4O_2 unit at this oxidation level was observed, although the product has not been isolated. Conversion of S_0 to S_1 and to S_2 thus requires no structural changes in the central Mn_4O_2 core, only electron abstraction, and possibly adjustment of peripheral ligation. On oxidation of S_2 to S_3, we now invoke a structural change. Water molecules bound to high oxidation state Mn atoms would be expected to be quite acidic and, on generation of S_3, we invoke a structural rearrangement brought about by deprotonation of the H_2O molecules and their conversion to bridging positions and, in the extreme, formation of a Mn_4O_4 cubane unit. The latter is actually depicted in Fig. 4 as $Mn_4O_2(OH)_2$ for reasons described below, but the former version is preferred, based on the tendency of high oxidation Mn to bind O^{2-} rather than OH^-.

Conversion of the Mn_4O_2 unit at S_2 to a Mn_4O_4 unit at S_3 requires little change in the positions of the constituent atoms. Note that the central Mn_2O_2 unit of the Mn_4O_2 structure is already half the cubic structure of the proposed S_3 structure; conversion of S_2 to S_3 thus requires only the slight movement towards each other of the two outer ('wing-tip') Mn atoms, each metal 'pivoting' about the μ_3-O^{2-} bridge, a motion requiring only an increase in the pyramidality of this O^{2-} ion.

The reason for invoking this structural rearrangement is based on the fact that coupling of two substrate molecules requires bringing them into close enough proximity such that subsequent oxygen–oxygen bond formation is facilitated allowing evolution of O_2. We estimate the $(H_2)O\ldots O(H_2)$ separation in S_2 to be about 4.5–5.0 Å. Structural conversion to S_3 now lowers the $(H)O\ldots O(H)$ separation to approx. 2.5 Å, a decrease of over 2 Å. The system is now poised for the all-important substrate-coupling reaction.

On oxidation of S_3 to unstable S_4, substrate oxidation is triggered. The O atoms move towards each other, initiating bond formation, and there is concomitant movement apart of the two Mn atoms, internal electron transfer from O to Mn

(and loss of any remaining H^+). An intermediate in this concerted process might be a peroxide-bound intermediate as depicted, at which point the O–O distance should be approx. 1.5–1.6 Å with a net of two electrons having been transferred to Mn. Continued approach of the two O atoms, transfer of two more electrons to the Mn and further movement apart of the latter leads to generation and evolution of O_2 and return of the remaining Mn_4O_2 unit back to S_0, in terms of both structure and oxidation level, ready for recycling. The indicated peroxide-bound intermediate requires electron transfer to take place in two two-electron steps rather than one four-electron step, but no intermediate has been observed in the S_3-to-S_0 transition and we are therefore not claiming the peroxide-bound form to be a stable intermediate but merely a transient during the substrate-coupling process. Note also that the overall formation of O_2 from the initially oxidized S_3 state represents a reductive elimination, a common process in inorganic chemistry but not, to our knowledge, well established to date for O_2 formation from bridging O^{2-} (or OH^-).

The complete scheme as depicted has two particularly attractive aspects in our opinion. One is that it is based, to a major extent, on species that are now established as capable of existence in a variety of oxidation levels, viz the Mn_4O_2-containing complexes. Two, the complete cycle requires little movement by the Mn/O framework. Indeed, the central Mn_2O_2 unit in the Mn_4O_2 species undergoes no movement at all and can be almost considered as possessing only a structural role.

The S_2-to-S_3 transition does, however, require some movement of the two outer Mn, but these

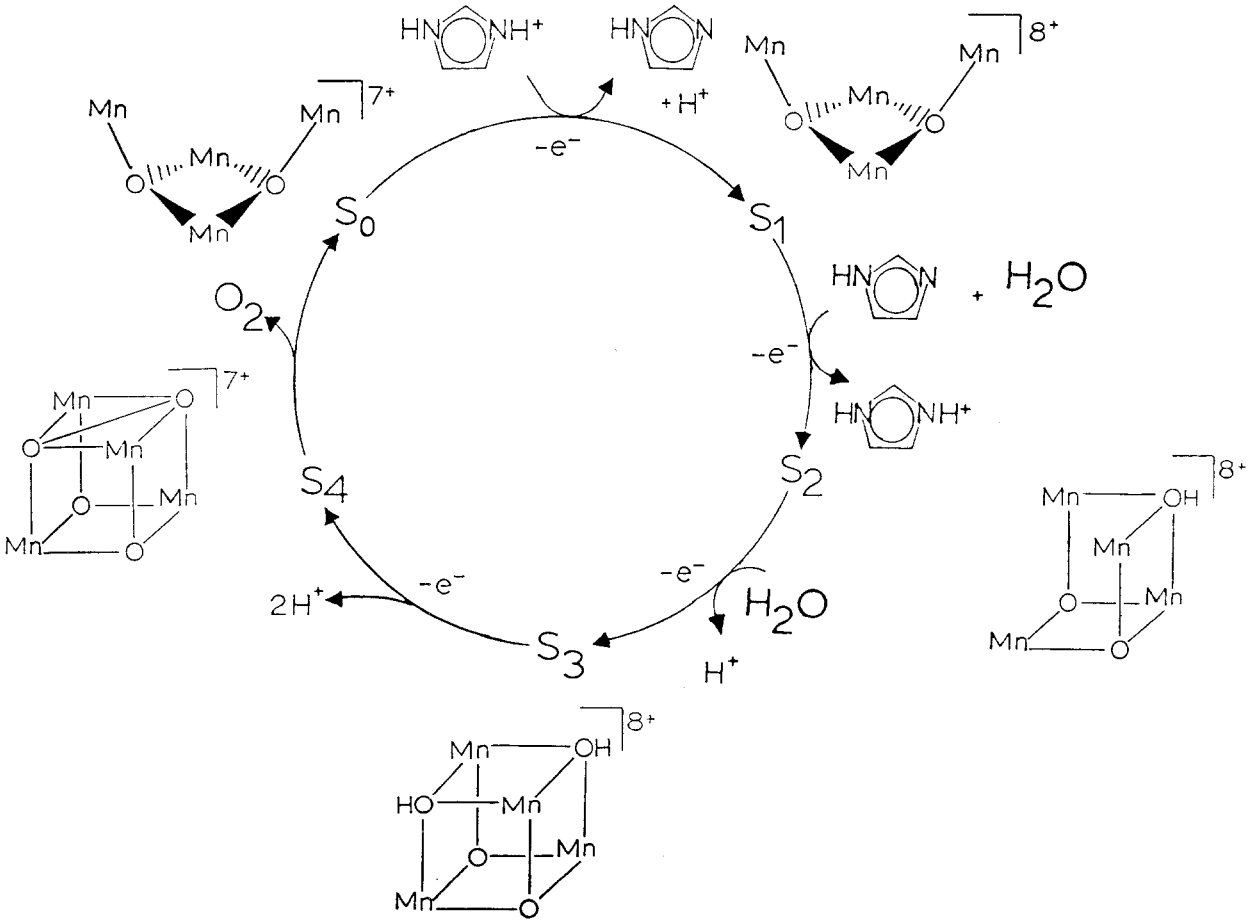

Fig. 5. Alternative mechanistic proposal for the water oxidation cycle; referred to as Scheme II in the text.

are minimal involving only fractions of an ångstrom. Overall, we feel only small reorganizational barriers will be introduced by our proposed scheme.

While the S_3 level depicted in Scheme I is shown as a cube with μ_3-oxides derived from substrate, there is no absolute requirement for μ_3-O^{2-} bridges, and a $Mn_4(\mu_3\text{-}O^{2-})_2(\mu_2\text{-}O^{2-})_2$ unit would be equally possible. The formation of such a unit would still require the same 'pivoting' about the μ_3-oxide bridges.

An alternative form of the scheme (Scheme II) can also be proposed, incorporating the now-established existence of the Mn_4O_3 core identified in complexes 4–6. This alternative scheme is depicted in Fig. 5 and differs only in the identity of the S_2 state [14]. Basically, instead of the two substrate molecules being bound in peripheral (terminal) positions to a S_2 Mn_4O_2 unit, we propose that one of them is deprotonated to OH^- or O^{2-} and is incorporated into the Mn_4O_2 unit, converting it to Mn_4O_3 or $Mn_4O_2(OH)$, as shown. (A second H_2O molecule may or may not also be bound in a terminal position, as in Scheme I.) This would require that pivoting of the Mn about the μ_3-O^{2-} groups occurs at the S_1-to-S_2 transition rather than at the S_2-to-S_3 transition, as in Scheme I. The μ_3-Cl^- seen in complexes 4–6 would occupy the remaining site of the Mn_4O_3 'partial cube', shown as vacant in Scheme II. This remaining site is subsequently occupied by the second deprotonated substrate molecule on oxidation of S_2 to S_3. In essence, the two schemes differ only in that in Scheme I incorporation of the two substrate molecules to yield the S_3 Mn_4O_4 unit occurs all at once during the S_2-to-S_3 transition, whereas in Scheme II the substrate molecules are incorporated sequentially during the S_1-to-S_2 and S_2-to-S_3 transitions; the possibility of sequential binding of substrate molecules by the native site has been discussed. Presently, the biophysical data on the enzyme do not allow clear preference for one of the two proposed schemes.

IV. Comparison with data on the native site

We now consider the proposed mechanisms in light of available biochemical and biophysical data accumulated on the native site.

IV.A. Nuclearity and manganese oxidation states

Below we review current data bearing on the question of the nuclearity of the native Mn cluster and the average metal oxidation state at each S_n. We will, in fact, begin by summarizing in advance the conclusions of this work, namely that the majority of current data support the cluster as being tetranuclear and the S_n states to contain the following Mn oxidation states:

S_{-1} $2Mn^{II},2Mn^{III}$
S_0 $Mn^{II},3Mn^{III}$
S_1 $4Mn^{III}$
S_2 $3Mn^{III},Mn^{IV}$
S_3 $2Mn^{III},2Mn^{IV}$

The only other reasonable possibility is that in which each S_n state has a two-unit increase in oxidation level; for example, S_1 would be $2Mn^{III},2Mn^{IV}$ and S_2 would be $Mn^{III},3Mn^{IV}$. Detailed EXAFS and edge studies have been reported, primarily on S_1 and S_2 [15]. Fits to the data lead to the following conclusions:

State	Mn-O_b [a] (Å)	Mn-O,N_t [b] (Å)	Mn...Mn (Å)
S_1	1.75(5)	2.00(5)	2.70(3)
S_2	1.76(5)	1.98(5)	2.72(3)

[a] Bridging ligands.
[b] Terminal ligands.

In addition, a fourth scattering shell has been assigned to a longer Mn...Mn separation of approx. 3.3 Å [16,17]. The two distinctly different Mn...Mn separations support both a nuclearity greater than two and significant asymmetry. Assuming tetranuclearity, these suggest either (i) two dinuclear units (Mn...Mn = 2.7 Å) separated by approx. 3.3 Å (no example currently known) or (ii) a dinuclear unit (Mn...Mn = 2.7 Å) with two additional Mn at approx. 3.3 Å but the latter themselves well separated. The 1.75 Å separation is indicative of bridging O^{2-} groups (or, conceivably, OH^-) and the approx. 2 Å separations indicative of terminally bound O/N-based ligands [15]. The EXAFS data thus suggest an asymmetrical, oxide-bridged Mn_4 cluster with peripheral

ligation provided by O/N-based ligands. Since no porphyrins are present, and available quinones have been assigned other functions [18], the peripheral ligands appear to be amino acid, side-chain functions viz carboxylate (glutamic/aspartic acids), phenoxide (tyrosine), imidazole (histidine), or combinations thereof. It can readily be seen that the Mn_4O_2 unit is in close correspondence with the EXAFS conclusions. Complex 2 consists of an asymmetrical, oxide-bridged array (type (ii) above) with both 'short' (2.85 Å) and 'long' (approx. 3.3 Å) separations, and peripherally ligated O/N-ligands.

EXAFS data on S_2 show little difference from S_1, suggesting little change in the basic coordination or structure during the S_1-to-S_2 transition [15]. Our proposal of a Mn_4O_2-unit at S_2 in Scheme I is thus consistent with this. Note, however, that EXAFS provides radial, not angular, information. Consequently, a small structural change could have occurred between S_1 and S_2 which, if no change in interatomic separations occurs, might yield the same EXAFS spectrum. Thus, the S_2 data could also be consistent with the Mn_4O_3-type unit indicated in Scheme II. The Mn_4O_3 cluster again possesses both 'short' (2.81 Å) and 'long' (approx. 3.3 Å) Mn...Mn separations and oxide bridges. It is our suggestion, therefore, that either a Mn_4O_2 or Mn_4O_3 unit (the latter with O/N peripheral ligands not Cl^- as in 4–6) could be at S_2 such that Scheme I or II cannot be preferred on this basis alone. Note also that fits of S_2 incorporating 1 Cl/4 Mn are equally as good as with no Cl [15], such that the entire Mn_4O_3Cl unit as seen in complexes 4–6 could indeed be present at S_2.

Additional support for a tetranuclear cluster derives from EPR fitting of the 'multiline' $g \approx 2$ EPR signal (vide infra). From a simulation study, it was concluded that the number of observed hyperfine lines (17–19) could not be arising from a dinuclear unit, but were instead due to a tetranuclear unit [19]. The simulations, however, could not distinguish between the possible oxidation levels at S_2 of $3Mn^{III},Mn^{IV}$ or $Mn^{III},3Mn^{IV}$. Additional attempts to simulate the hyperfine structure have been reported [44]. Introduction of g-anisotropy was necessary to adequately simulate the X-band spectrum; however, the authors point out that the parameters obtained were unable to simulate the Q-band spectrum correctly [29]. The anisotropy is also inconsistent with orientation dependence studies [26] and studies using variable microwave frequencies [29]. Consequently, the inability to simulate the multiline signal with Mn_2 models suggests inclusion of contributions from additional Mn atoms may be necessary. See also Ref. 74 for recent additional comments concluding a nuclearity greater than 2. The EPR spectrum of complex 4 displays a $g \approx 2$ signal with 16 hyperfine lines [12]; signal-to-noise is currently too great, due to low solubility, to allow any additional lines in the wings to be observable (if present), but does establish for the first time that a synthetic tetranuclear $3Mn^{III},Mn^{IV}$ cluster can yield a spectrum somewhat similar to S_2.

^{1}H-NMR has also been used as a probe for the Mn oxidation levels in the S_n states. The studies involved measuring the solvent water relaxation rates as a function of S_n state. The observed rates at each S_n showed the order $S_0 > S_1 < S_2$ and the authors concluded that the S_0-to-S_1 transition involves a $Mn^{II} \rightarrow Mn^{III}$ oxidation, whereas the S_1-to-S_2 transition involves a $Mn^{III} \rightarrow Mn^{IV}$ oxidation [20]. Inherent in this analysis was the assumption that the Mn atoms within the cluster are only weakly coupled such that they behave as isolated Mn ions. This may or may not be a safe assumption, but the experimental results seem nevertheless correct for they are supported by other studies. For example, measurement by EPR spin echo of the relaxation rates of D^+ (the phenoxide radical of Tyr-160 of polypeptide D_2) [6] shows that the relaxation rates again display the pattern $S_0 > S_1 < S_2$ [21]. If the cluster cannot be considered as four, only weakly coupled Mn ions, then the relaxation rates should parallel the overall paramagnetic susceptibility of the cluster, suggesting that the cluster magnetic moments should also be $S_0 > S_1 < S_2$. Recent studies have probed the magnitude of the moments and values of μ^2 have been concluded to show the same pattern, viz $S_1 < S_2$ [22]. These three different studies thus all lead to the same conclusion. Interestingly, the room temperature moments of our S_0, S_1 and S_2 model complexes expressed as μ^2 display this same pattern viz $S_0 > S_1 < S_2$. In addition, the magnitude of $\Delta\mu^2$ for the transition S_1-to-S_2 is approx. + 13, which agrees surprisingly well with the $\Delta\mu^2$ for

complexes 3 and 5 ($\Delta\mu^2 = +14.4$). Such an increase in μ^2 is not that expected for a simple dinuclear unit being oxidized from a Mn_2^{III} (S_1) to a $Mn^{III}Mn^{IV}$ (S_2) level, for the greater magnetic coupling expected in the latter complexes compared with the former would be expected to lead to a decrease in μ^2 on the S_1-to-S_2 transition; i.e., $\Delta\mu^2$ would be negative. The increase in μ^2 in 5 arises from a mixture of antiferromagnetic coupling between the Mn^{III}-Mn^{IV} pairs and ferromagnetic coupling between the Mn^{III}-Mn^{III} pairs [13]. Such a coupling scheme also likely occurs for the Mn assembly in the S_2 level [19,27].

Difference UV/visible spectra have also been measured during the transitions $S_0 \rightarrow S_1 \rightarrow S_2 \rightarrow S_3$. After some initial disagreements from different laboratories, the majority have now reached a consensus, viz the S_0-to-S_1 transition yields a distinctly different spectrum to the S_1-to-S_2 and S_2-to-S_3 transitions while the latter two display the same difference spectra [23–25]; one study, however, reports the latter two spectra to be different [13]. The conclusion is that a distinctly different process is occurring for S_0-to-S_1 compared to subsequent oxidations, and the authors have assigned S_0-to-S_1 as involving a $Mn^{II} \rightarrow Mn^{III}$ oxidation, whereas S_1-to-S_2 and S_2-to-S_3 each involve a $Mn^{III} \rightarrow Mn^{IV}$ oxidation. Our proposed S_0 and S_1 model complexes 2 and 3 display a difference spectrum extremely similar in band position and profile to the native S_0-to-S_1 difference spectrum and different from those for the subsequent oxidations (Fig. 6).

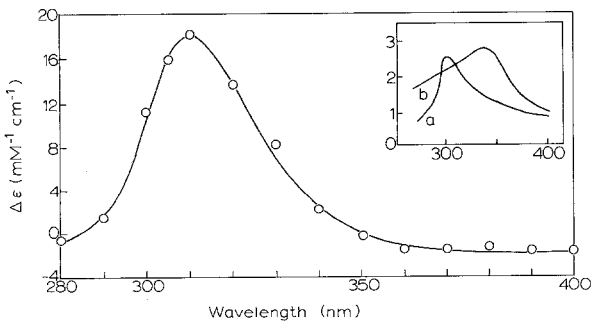

Fig. 6. The UV/vis difference spectrum for the $[Mn_4O_2(O_2CR)_7(bipy)_2]^{0,+}$ pair (complexes 2 and R = Ph analogue of 3). The inset contains the difference spectra for the S_0/S_1 (a) and S_1/S_2 and S_2/S_3 (b) transitions (taken from Ref. 24).

As we noted earlier, four Mn are needed in simulating the number of hyperfine lines in the 'multiline' EPR signal of S_2. Additional support comes from the temperature dependence of this signal's non-Curie-like behavior [22,28], inconsistent with a dinuclear species. Other workers have, however, reported Curie-like behavior for their samples [29]. The differences observed in the temperature dependence studies have been shown to be a function of the cryoprotectant used, for reasons which are currently unclear [44]. Fitting of the temperature dependence data with the model recently developed for 5 [75], the only characterized $Mn_3^{III}Mn^{IV}$ complex, could prove useful.

A combination of studies has been reported which bears on the question of the Mn oxidation levels at S_{-1}, the most reduced, stable form of the cluster. Treatment of S_1 with H_2O_2 yields S_{-1} which requires five flashes of light before O_2 is generated [30]. That H_2O_2 is not degrading the cluster during the reduction and the cluster is reformed during the subsequent reoxidation is supported by careful studies employing low concentrations of H_2O_2 which show that no free Mn^{2+} is generated [31]. Thus, a cluster which still maintains its integrity is indicated, and based on S_1 containing $4Mn^{III}$, S_{-1} must contain $2Mn^{II},2Mn^{III}$. Attempts to reduce further than S_{-1} now lead to observation of liberated free Mn^{2+}, suggesting S_{-1} is indeed the most reduced level the cluster can adopt without degradation [32].

Studies from the 'opposite direction' have also been performed. Using particles which have been depleted of all Mn, the reincorporation of added Mn^{2+} has been studied [33,34]. No reactivation is observed without flashes of light being administered. On one flash, one Mn^{2+} is oxidized and attached. A second flash of light leads to incorporation of a second Mn^{3+} and, spontaneously, the incorporation of two further Mn^{2+}. Since only two flashes of light are needed for this photoreactivation process, and each flash leads to a one-electron charge separation at the reaction center, the apparent implication is that the four Mn atoms have been reincorporated as $2Mn^{II},2Mn^{III}$. Although the S_n state thus formed has not been identified, it seems reasonable to suspect that this is S_{-1}. It must now be determined how many additional flashes are required to generate the

EPR-active S_2 state; our arguments suggest that this will be three ($S_{-1} \rightarrow S_2$).

The results of our synthetic work are in accord with the above reduction and reactivation experiments. The lowest oxidation level we have been able to generate for our synthetic Mn_4 complexes is $2Mn^{II},2Mn^{III}$ corresponding to S_{-1}. Further reduction (with NH_2OH, etc.) leads to degradation. We believe these parallel observations support our contention that the Mn_4O_2 units may well indeed represent the units to be found in the native site at the lower S_n states.

Some general inorganic chemistry comments seem to be warranted at this point. It has often been argued by workers preferring the alternative oxidation state description (i.e., S_1 is $2Mn^{III},2Mn^{IV}$ and therefore S_{-1} is $4Mn^{III}$) that this avoids the presence of Mn^{II} at any S_n state, and that this is essential because Mn^{2+} is known to be labile and its generation in lower S_n states would lead to the cluster 'falling apart'. This is inconsistent with the variety of data briefly reviewed above indicating Mn^{II} at lower S_n states and also is not supported by the inorganic chemistry of this metal. While mononuclear Mn^{II} is indeed labile, its incorporation within mixed valence, oxo-bridged clusters leads to stable species. Thus, mixed-valence Mn^{II},Mn^{III} species have been found for dinuclear, trinuclear (Mn_3O^{6+}) and, of course, the tetranuclear ($Mn_4O_2^{6+,7+}$) complexes 1 and 2. It is, therefore, not valid to argue that no Mn^{II} can be present at the lower S_n states; both the data on the native site and Mn inorganic chemistry support the alternative belief.

In summary, the majority of data support the native site to consist of a tetranuclear Mn cluster. Further, available data support the Mn oxidation-state assignments specified earlier or cannot distinguish between it and the alternative assignment. Further, the synthetic species containing Mn_4O_2 and Mn_4O_3 units are in satisfactory agreement at the present time with native data in terms of nuclearity, ligation type, structural parameters, oxidation levels and spectroscopic properties.

IV.B. EPR data and substrate binding

Oxidation of S_1 to S_2 at approx. 190 K or above, by a single flash of light, generates the familiar $g \approx 2$ EPR signal of S_2, which possesses Mn hyperfine structure (17–19 lines) and is referred to as the 'multiline' signal [35]. If, however, the oxidation is performed at 130 K, a different signal centered at $g \approx 4$ is obtained instead [36–38]. On warming this sample, the $g \approx 4$ signal decays and is replaced by the multiline spectrum [39]. These results were originally interpreted as indicating an $S = 3/2$ ground state ($g \approx 4$) with an $S = 1/2$ excited state ($g \approx 2$) [39]. However, it has since been reported that these two species may not be arising from differing thermal populations of the same cluster [29].

Substrate binding to S_2 has been probed by investigating the appearance of the multiline in the presence of ^{17}O, H_2O and ^2H_2O. The former shows broadening of the multiline signal when generated at approx. 210K [40]. This would suggest binding of labeled H_2O at the substrate binding site or bridging oxide exchange with labeled H_2O with no binding of H_2O at the substrate site; oxide exchange between labeled H_2O and bridging O^{2-} has been shown in synthetic dinuclear Mn oxide-bridged complexes [41,42]. The ^2H_2O experiments at both 200 K and 10 °C also show sharpening of the multiline signal, however, suggesting that water is bound at the substrate binding site at S_2 [43]. Taken together, these results imply the form of S_2 yielding the multiline signal is able to bind substrate molecules. Our S_2 models depicted in Schemes I and II are consistent with this, as will be described. Whether water is bound at S_1, however, is currently not as clear.

(a) If no H_2O is bound to S_1, we suggest the $g \approx 4$ signal might arise by oxidation to S_2 but, due to the low temperatures, water cannot bind and therefore the normal multiline signal is not observed, i.e., the $g \approx 4$ signal is the cluster without bound substrate, whereas the $g \approx 2$ signal is the cluster with bound substrate. The substrate-bound form could be either as depicted in Scheme I (H_2O molecules in peripheral positions) or in Scheme II (one H_2O incorporated to give a Mn_4O_3 unit; a second H_2O could or could not be bound in a peripheral position).

(b) If H_2O is bound at S_1 or H_2O binding can occur at 130 K, the $g \approx 4$ species could be merely the same Mn_4O_2 unit (with bound H_2O) at a higher oxidation level, which cannot undergo any

structural change due to the low temperature. The $g \approx 2$ species could then be for example the Mn_4O_3 unit, i.e., the required structural change has now occurred.

For both possibilities (a) and (b), warming the $g \approx 4$ species now allows either the H_2O binding or the structural change that the low temperatures have blocked. It has been reported that the conversion of the $g \approx 4$ to the $g \approx 2$ species involves an associative process (ΔS negative) [44]; both a substrate binding and a structural change would be consistent with this. X-ray absorption edge studies of the species giving rise to the two ESR signals indicate that the species can only differ subtly [15], perhaps favoring (a).

Also note that continuous illumination of the $g \approx 4$ species at low temperatures does not yield any S_3 or O_2 evolution. Again, both the absence of bound substrate or the blocking of the Mn_4O_2 to Mn_4O_3 conversion would be consistent with this, for formation of the S_3-type cluster in Schemes I and II would itself be blocked.

A parallel series of experiments has been performed in the presence of NH_3 as a potential substrate analog. The various data obtained are more difficult to interpret and, as a result, their rationalization by or consistency with our proposed mechanisms is more difficult to gauge. Nevertheless, we shall attempt a partial rationalization.

Generation of S_2 at $-10\,^\circ C$ in the presence of NH_3 yields a 'modified' multiline ($g \approx 2$) signal, suggesting NH_3 has bound at the subtrate binding site [45]. However, generation of S_2 at 210 K yields instead a mixture of the normal $g \approx 4$ signal and the normal $g \approx 2$ signal, suggesting NH_3 is not bound [45,46]. Incubation of this sample, however, at $0\,^\circ C$ leads to the 'modified' $g \approx 2$ signal, suggesting NH_3 is now bound. While such behavior is open to detailed interpretation in several ways, we would propose the following: (a) these studies would argue against any H_2O being bound at S_1, for one would reasonably assume that NH_3 would also bind at S_1 and would remain bound at S_2, yielding modified S_2 $g \approx 4$ or $g \approx 2$ signals, even when generated at low temperatures; (b) generation of S_2 at 210 K leads to a mixture comprising the $g \approx 4$ species (as described above) and the normal multiline ($g \approx 2$) species representing the H_2O-bound form (Mn_4O_2 with peripherally bound H_2O as in Scheme I or Mn_4O_3 as in Scheme II). Why water might bind at 210 K or lower but not NH_3 can be possibly rationalized on the basis that the concentration of H_2O molecules is vastly greater than the concentration of NH_3. Basically, the normal multiline seen at 210 K could represent a kinetic product, the lower temperature of the glass slowing NH_3 binding which would represent formation of the thermodynamic product, the latter occurring at higher temperatures. It would be interesting to know whether long-term storage of the S_2 sample generated at 210 K slowly converts to the 'modified' multiline of the NH_3-bound form; to our knowledge, this experiment has not been performed.

The identity of the species yielding the modified multiline signal could be either an Mn_4O_2-unit with peripheral NH_3 (the S_2 model of Scheme I with NH_3 in place of H_2O) or a Mn_4O_3 (as in Scheme II) with peripherally bound NH_3. Note that preformed normal $g \approx 2$ spectra are converted to the modified form on subsequent addition of NH_3; according to Scheme I, this would simply be exchange of H_2O by NH_3, whereas for Scheme II, this could be binding of NH_3 to a vacant site on the Mn_4O_3 unit or displacement of a peripherally bound H_2O.

In the presence of NH_3, O_2 evolution is blocked [47]. Again, we can possibly rationalize this as being due to the inability of generating the S_3 structure; NH_3 is much less acidic than H_2O and its deprotonation to NH_2^- is thus extremely unlikely; it therefore cannot allow the corresponding NH_2^--bridged S_3-type structure to form, and being bound instead of H_2O molecules does not allow the latter to mediate formation of the S_3 cluster either. Consequently, O–O bond formation is blocked on subsequent oxidation. Along the same lines, note that binding of NH_3 to preformed S_2 at high temperatures is rapid, but its binding to preformed S_3 is very slow [47]. This might be due to the need to disrupt the indicated S_3 cluster, displacing the bridging O^{2-} (or OH^-), i.e., a seriously perturbed or abnormal S_3 structure is generated, one not lying on the normal catalytic cycle.

Further evidence suggesting the incorporation of substrate water at the S_2 level comes from

investigation of the temperature dependence of S-state transition kinetics [48]. The activation entropy for the S_1-to-S_2 transition is considerably more negative than for the S_2-to-S_3 transition, indicating more ordering for the first transition. This would be consistent with the binding of substrate water at the S_2 level or incorporation of a molecule of water and pivoting of an Mn_4O_2 unit to the Mn_4O_3 core. Also, the potential for the oxidation of the synthetic $Mn(III)_4O_2$ complex is higher than that of the oxidant of the biological manganese. This suggests that a mechanism for reducing this redox potential such as the binding of H_2O or ammonia or incorporation of an additional bridging oxide is necessary to generate an Mn_4O_2-based complex at the S_2 oxidation level.

IV.C. Miscellaneous data

Mass spectral studies employing ^{18}O water have led to the conclusion that no intermediate oxidation state products of H_2O are generated during the S_n state advancement to S_3 [49,50]. This implies all substrate oxidation occurs during the final S_3-to-S_0 transition. For that reason, both forms of our mechanism show only changes to the protonation of the substrates, not their oxidation level.

The observed proton release pattern during the S-state advancement $S_0 \rightarrow S_1 \rightarrow S_2 \rightarrow S_3 \rightarrow S_0$ is 1,0,1,2 [51]. Of course, this may not correspond to the actual proton release from H_2O, for they could be transferred from H_2O to basic sites in the environment. Nevertheless, we have adjusted our schemes to be consistent with this pattern and show, for instance, some S_n states possessing bridging OH^- instead of O^{2-}; we actually prefer the latter. Also, we invoke in some steps the involvement of amino acid side-chain functions such as the indicated histidine to function as proton acceptor sites [52,53]. We emphasize, however, that although we have adjusted our schemes to be consistent with the observed proton release pattern, this is done only tentatively, for the elucidation of the precise movement and fate of protons in such a complex system is likely to require much more detailed and sophisticated study.

The water oxidation activity is known to require Cl^- although other simple anions can be substituted with retention of activity [2,3]. Most current evidence suggests the Cl^- binding sites are not the Mn centers [54,46] but the identification of complexes 4–6 containing a μ_3-Cl^- in the Mn_4O_3 central unit is intriguing. It is tempting to speculate that our proposed S_2 model in Scheme II is actually a Mn_4O_3Cl unit, the Cl^- being displaced by the subsequent incorporation of another O^{2-} (or OH^-) during conversion to S_3. Note that EXAFS fits do not rule out 1 Cl/4 Mn. It is also interesting that Cl^--depleted systems yield an S_2 state exhibiting a $g \approx 4$ signal and which cannot be further oxidized [55,56]. Within the framework of our mechanisms, one could interpret this as blocking the formation of the Mn_4O_3 unit in Scheme II by either precluding formation of Mn_4O_3Cl or by blocking any subtle conformational changes needed to accommodate formation of Mn_4O_3 from Mn_4O_2. Alternatively, for Scheme I, blocking of conformational changes required to allow access of H_2O to the Mn site would yield a Mn_4O_2 unit without bound H_2O and unable to advance to S_3.

The function of D^+ seems to be to oxidize S_0 to S_1 during periods of dark adaptation [57,58], possibly suggesting that S_1 is more stable than S_0 and a defense mechanism operates to prevent the long-term existence of S_0. We have no argument with this contention as long as it is based on relative stabilities. As we discussed earlier, mixed valence $Mn^{II}Mn^{III}$ clusters are not intrinsically unstable. Additionally, we do not see the need for the D^+ oxidation of S_0 if the latter were $3Mn^{III},Mn^{IV}$; indeed, we view the function of D^+ to lend additional support to the presence of Mn^{II} at S_0.

IV.D. Location of the Mn cluster

Current evidence from studies of a mutant cyanobacterium (with the oxidizing side of its PS II reaction center blocked [59,60]), and from iodination studies [61] has associated the D1 membrane protein (albeit circumstantially) with manganese. Additionally, a cross-linked polypeptide complex composed of D1, D2, and a 33 kDa extrinsic polypeptide retains bound Mn [62]. As the extrinsic protein can be washed from PS II reaction centers with retention of Mn [63], this

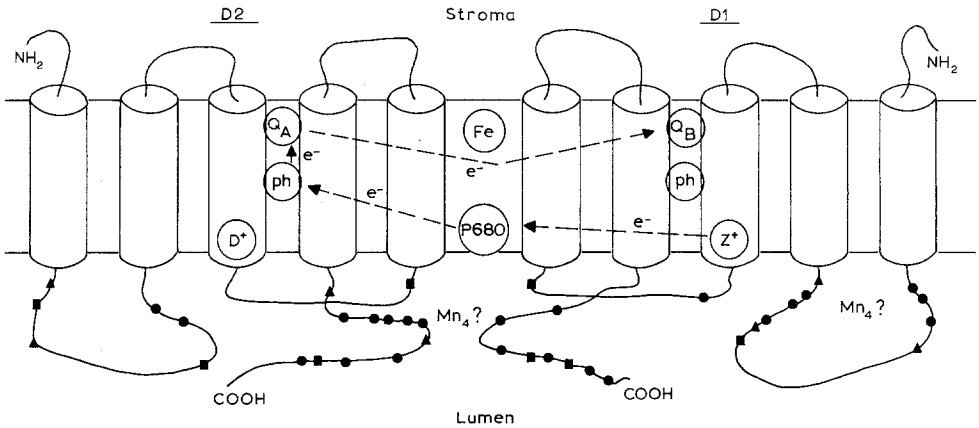

Fig. 7. Diagrammatic representation of the P-680 (PS II) reaction center (ph = pheophytin). The dashed line shows the presumed electron transfer pathway to quinone Q_B. The two potential locations of an Mn_4 cluster in a carboxylate-rich region are shown (■ = histidine, ● = aspartic or glutamic acids, ▲ = tyrosine).

suggests the bulk of the Mn ligation to be provided by the D1 and D2 proteins. The amino acid sequences of these proteins have been determined from a number of cyanobacteria and plants [64–66]. Based on the homology of these two proteins and the L and M subunits of bacterial reaction centers (two of which have been characterized by X-ray crystallography [67,68]), the folding patterns of D1 and D2 have been predicted and recently confirmed by site-directed antisera studies [69,70]. As the manganese has been shown to be limited to the lumenal side of the thylakoid membrane, the recent prediction of the D1 and D2 structures allows probable manganese binding sites to be identified. For the spinach proteins, 23 glutamate or aspartate, 8 histidine, and 7 tyrosine residues are exposed to the lumen [4]; thus, ligation of the photosynthetic manganese might be primarily through the carboxylate functionalities of glutamate and aspartate residues. In the case of the synthetic complexes with Mn_4O_2 cores, at least six carboxylates have always been found to be ligated. Two carboxylate-rich sites can be identified on the D1 and D2 polypeptides: (1) on the carboxy termini of the D1 and D2 polypeptides which retain the C_2 symmetry believed to be present in the PS II reaction center and (2) on the region of the D2 polypeptide connecting the first two transmembrane helices from the amino terminus. Based on the position of Z^+ (presumably tyrosine 161 of D1 [6] and the electron acceptor to the Mn assembly), we prefer the latter. The above comments are summarized pictorially in Fig. 7.

IV.E. Carboxylate substitution and cluster extrusion

One property of complex 3 which is of potential biological significance is its ability to undergo facile carboxylate exchange. Thus, treatment of a solution of $[Mn_4O_2(OAc)_7(bipy)_2]^+$ with excess RCOOH (R = H, Ph) leads to quantitative conversion to $[Mn_4O_2(O_2CR)_7(bipy)_2]^+$. This is analogous to the thiolate substitution reactions exhibited by the $[Fe_4S_4(SR)_4]^{2-}$ clusters which are models of the ferredoxin proteins. For the latter, this has allowed the 'core extrusion' reaction

$$Fe_4S_4(pep) + xs\ PhSH \rightarrow [Fe_4S_4(SPh)_4]^{2-} + pepH_4$$

to be developed as shown below where $pepH_4$ is the ferredoxin apoprotein [71]. Thus, the Fe/S cluster can be extracted or 'extruded' from its native environment.

The observation of facile carboxylate exchange by more acidic carboxylic acids in complex 3 suggests a similar reaction may be possible with the Mn cluster. Thus, treatment of chloroplast particles under appropriate conditions with excess carboxylate reagents (and bipyridine ?) might allow extraction of the native cluster in a form peripherally ligated by small ligands rather than

the native polypeptides (D_1, D_2, etc.). Indeed, we were intrigued by the observation that high concentrations of acetate destroy water oxidation activity. It was proposed that this was due to competition by acetate for the substrate or Cl^- binding sites [72]. Might it have instead been due to partial displacement of the cluster from its binding polypeptides? On removal of the acetate, the water oxidation activity is regained; this would be consistent with the polypeptides reattaching the Mn_4 cluster by re-displacing the bound carboxylates. Recent studies have additionally shown that acetate treatment leads to uncoupling of the Mn complex from its electron acceptor [73]. It will be interesting to see if conditions can be found for treating chloroplast particles with small carboxylates, and whether a Mn_4 unit can be then extracted into non-aqueous solvents, for example, to allow spectroscopic comparisons with available synthetic materials.

V. Conclusions

Elucidating the structure and mechanism of action of such a complex system as the water oxidation center represents a challenge of some magnitude. It certainly requires a variety of techniques and expertise to be brought to bear on the problem, not least of which is inorganic chemistry. While our work in this area is still in its early days, a pool of synthetic complexes has already been assembled and they have allowed initial mechanistic proposals to be offered for consideration. They may or may not prove to be related to the native system and will, in any case, no doubt be modified as work progresses and more data become available; such is the nature of hypothetical proposals in Science. At the very least, the proposals are based largely on established Mn complexes that should therefore, we believe, be entertained as candidates for the metal units evolved to be present in the native system. Of course, the described complexes represent the initial products of our efforts, and different structural types may well result from work in progress. At such time as the latter are obtained (and should they prove to be attractive as models) their potential incorporation into alternative or preferable mechanistic schemes will be evaluated. In the meantime, we refrain from alternative mechanisms based on purely hypothetical complexes, preferring as we stated in the Introduction to employ as much as possible structural types known to exist. Further work in progress is directed towards both the synthesis of the structural unit proposed at S_3, and the investigation of any other structural types capable of existence at these oxidation levels and with the appropriate, biologically-relevant ligands.

Acknowledgements

Research in this area was generously supported by NSF (CHE 8507748) and NIH (GM39083-1), and funds available through an Alfred P. Sloan Fellowship (1987-1992) and a Camille and Henry Dreyfus Teacher-Scholar Grant to G.C.

References

1 Amesz, J. (1983) Biochim. Biophys. Acta 726, 1–12.
2 Govindjee, Kambara, T. and Coleman, W. (1985) Photochem. Photobiol. 42, 187–210.
3 Dismukes, G.C. (1986) Photochem. Photobiol. 43, 99–115.
4 Trebst, A. (1986) Z. Naturforsch 41C, 240–245.
5 Michel, H. and Deisenhofer, J. (1988) Biochem. 27, 1–7.
6 Debus, R.J., Barry, B.A., Babcock, G.T. and McIntosh, L. (1988) Proc. Natl. Acad. Sci. USA 85, 427–430.
7 Brudvig, G.W. and Crabtree, R.H. (1986) Proc. Natl. Acad. Sci. USA 83, 4586–4588.
8 Vincent, J.B. and Christou, G. (1987) Inorg. Chim. Acta 136, L41–L43.
9 Kok, B., Forbush, B. and McGloin, M. (1970) Photochem. Photobiol. 11, 457–475.
10 Vincent, J.B., Christmas, C., Huffman, J.C., Christou, G., Chang, H.-R. and Hendrickson, D.N. (1987) J. Chem. Soc., Chem. Commun., 236–238.
11 Christmas, C., Vincent, J.B., Huffman, J.C., Christou, G., Chang, H.-R. and Hendrickson, D.N. (1987) J. Chem. Soc., Chem. Commun., 1303–1305.
12 Bashkin, J.S., Chang, H.-R., Streib, W.E., Huffman, J.C., Hendrickson, D.N. and Christou, G. (1987) J. Am. Chem. Soc. 109, 6502–6504.
13 Lavergne, J. (1987) Biochim. Biophys. Acta 894, 91–107.
14 Christou, G. and Vincent, J.B. (1988) in Metal Clusters in Proteins; (Que, L., ed.), ACS Symposium Series 372, Ch. 12, American Chemical Society, Washington, D.C.
15 Yachandra, V.K., Guiles, R.D., McDermott, A.E., Cole, J.L., Britt, R.D., Dexheimer, S.L., Sauer, K. and Klein, M.P. (1987) Biochem. 26, 5974–5981.
16 Guiles, R.D., Yachandra, V.K., McDermott, A.E., Britt, R.D., Dexheimer, S.L., Sauer, K. and Klein, M.P. (1987) in Progress in Photosynthesis Research (Biggins, J., ed.), Vol. I, pp. 561–564, Martinus Nijhoff, Dordrecht.
17 George, G.N., Prince, R.C. and Cramer, S.P. (1987) 14th Annual User's Conference Stanford Synchrotron Radiation Laboratory, SSRL Report No. 87/05, p. 10, Stanford University, Stanford, CA.

18 Ohno, T., Satoh, K. and Katoh, S. (1986) Biochim. Biophys. Acta 852, 1–8.
19 Dismukes, G.C., Ferris, K. and Watnick, P. (1982) Photobiochem. Photobiophys. 3, 243–256.
20 Srinivasan, A.N. and Sharp, R.R. (1986) Biochim. Biophys. Acta 851, 369–376.
21 Hoff, A.J., Evelo, R., Styring, S. and Rutherford, A.W. (1987) Rec. Trav. Chim. Pays-Bay 106, 215.
22 Dismukes, G.C. (1987) (a presentation at the) Royal Society of Chemistry IBDG Meeting, King's College, London, December 1987.
23 Dekker, J.P., Van Gorkom, H.J., Brok, M. and Ouwehand, L. (1984) Biochim. Biophys. Acta 764, 301–309.
24 Saygin, O. and Witt, H.T. (1987) Biochim. Biophys. Acta 893, 452–469.
25 Kretschmann, H., Dekker, J.P. Saygin, O. and Witt, H.T. (1988) Biochim. Biophys. Acta 932, 358–361.
26 Rutherford, A.W. (1985) Biochim. Biophys. Acta 807, 189.
27 De Paula, J.C., Beck, W.F. and Brudvig, G.W. (1986) J. Am. Chem. Soc. 108, 4002–4009.
28 Dismukes, G.C. and Damoder, R. (1985) Biophys. J. 47, 166a.
29 Hansson, O., Aasa, R. and Vänngård, T. (1987) Biophys. J. 51, 825–832.
30 Velthuys, B. and Kok, B. (1978) Biochim. Biophys. Acta 502, 211–221.
31 Frasch, W.D. and Mei, R. (1987) Biochim. Biophys. Acta 891, 8–14.
32 Beck, W.F. and Brudvig, G.W. (1987) Biochem. 26, 8285–8295.
33 Tamura, N. and Cheniae, G. (1987) Biochim. Biophys. Acta 890, 179–194.
34 Ono, T.-a. and Inoue, Y. (1987) Plant Cell Physiol. 28, 1293–1299.
35 Dismukes, G.C. and Siderer, Y. (1980) FEBS Lett. 121, 78–80.
36 Casey, J.L. and Sauer, K. (1984) Biochim. Biophys. Acta 723, 361–371.
37 Zimmerman, J.-L. and Rutherford, A.W. (1984) Biochim. Biophys. Acta 767, 160–167.
38 Zimmerman, J.-L. and Rutherford, A.W. (1986) Biochem. 25, 4609–4615.
39 De Paula, J.C., Beck, W.F. and Brudvig, G.W. (1986) J. Am. Chem. Soc. 108, 4002–4009.
40 Hansson, O., Andréasson, L.-E. and Vänngård, T. (1986) FEBS Lett. 195, 151–154.
41 Cooper, S.R. and Calvin, M. (1977) J. Am. Chem. Soc. 99, 6623–6630.
42 Sheats, J.E., Czernuszewicz, R.S., Dismukes, G.C., Rheingold, A.L., Petrouleas, V., Stubbe, J., Armstrong, W.H., Beer, R.H. and Lippard, S.J. (1987) J. Am. Chem. Soc. 109, 1435–1444.
43 Nugent, J.H.A. (1987) Biochim. Biophys. Acta 893, 184–189.
44 De Paula, J.C., Beck, W.F., Miller, A.-F., Wilson, R.B. and Brudvig, G.W. (1987) J. Chem. Soc., Faraday Trans 83, 3635–3651.
45 Beck, W.F., De Paula, J.C. and Brudvig, G.W. (1986) J. Am. Chem. Soc. 108, 4018–4022.
46 Beck, W.F. and Brudvig, G.W. (1986) Biochem. 25, 6479–6486.
47 Velthuys, B.R. (1975) Biochim. Biophys. Acta 396, 392–401.
48 Koike, H., Hanssum, B., Inoue, Y. and Renger, G. (1987) Biochim. Biophys. Acta 893, 524–533.
49 Radmer, R. and Ollinger, O. (1986) FEBS Lett. 195, 285–289.
50 Bader, K.P., Thibault, P. and Schmid, G.H. (1987) Biochim. Biophys. Acta 893, 564–571.
51 Forster, V. and Junge, W. (1985) Photochem. Photobiol. 41, 183–190.
52 Homann, P.H. (1985) Biochim. Biophys. Acta 809, 311–319.
53 Coleman, W.J., Govindjee and Gutowsky, H.S. (1987) Biochim. Biophys. Acta 894, 443–452.
54 Yachandra, V.K., Guiles, R.D., Sauer, K. and Klein, M.P. (1986) Biochim. Biophys. Acta 850, 333–342.
55 Ono, T.-a., Nakayama, H., Gleiter, H., Inoue, Y. and Kawamori, A. (1987) Arch. Biochem. Biophys. 256, 618–624.
56 Vass, I., Ono, T.-a. and Inoue, Y. (1987) Biochim. Biophys. Acta 892, 224–235.
57 Styring, S. and Rutherford, A.W. (1987) Biochem. 26, 2401–2405.
58 Nugent, J.H.A., Demetriou, C. and Lockett, C.J. (1987) Biochim. Biophys. Acta 894, 534–542.
59 Metz, J.G. and Seibert, M. (1984) Plant Physiol. 76, 829–832.
60 Rutherford, A.W., Seibert, M. and Metz, J.G. (1988) Biochim. Biophys. Acta 932, 171–176.
61 Ikeuchi, M., Koike, H. and Inoue, Y. (1988) Biochim. Biophys. Acta 932, 160–169.
62 Bowlby, N.R. and Frasch, W.D. (1987) in Progress in Photosynthesis Research (Biggins, J., ed.), Vol. I, pp. 693–696, Martinus Nijhoff, Dordrecht.
63 Ono, T. and Inoue, Y. (1983) FEBS Lett. 164, 255–260.
64 Alt, J., Morris, J., Westhoff, P. and Herrman, R.G. (1984) Cur. Gen. 8, 597–606.
65 Kyle, D.J. (1985) Photochem. Photobiol. 41, 107–116.
66 Rochaix, J.-D., Oron, M., Rahire, M. and Malnoe, P. (1984) Plant Mol. Biol. 180, 385–398.
67 Deisenhofer, J., Epp, O., Miki, K., Huber, R. and Michel, H. (1985) Nature 318, 618–624.
68 Allen, J.P., Feher, G., Yeates, T.O., Komiya, H. and Rees, D.C. (1987) Proc. Natl. Acad. Sci. USA 84, 6162–6166.
69 Geiger, R., Berzborn, R.J., Depka, B., Oettmeier, W. and Trebst, A. (1987) Z. Naturforsch 42C, 491–498.
70 Sayre, R.T., Andersson, B. and Bogorad, L. (1986) Cell 47, 601–608.
71 Berg, J.M., Holm, R.H. (1982) in Iron-Sulfur Proteins (Spiro, T.G., ed.), Ch. 1, Wiley, New York.
72 Saygin, O., Gerken, S., Meyer, B. and Witt, H.T. (1986) Photosyn. Res. 9, 71–78.
73 Bock, C.H., Gerken, S., Stehlik, D. and Witt, H.T. (1988) FEBS Lett. 227, 141–146.
74 Brudvig, G.W. (1988) in Metal Clusters in Proteins (Que, L., ed.), ACS Symposium Series 372, Ch. 11, American Chemical Society, Washington, DC.
75 Li, Q., Vincent, J.B., Libby, E., Chang, H.-R., Huffman, J.C., Boyd, P.D.W., Christou, G. and Hendrickson, D.N. (1988) Angew. Chem. Int. Ed. Engl., in press.